Dynamic mechanical response of ZrCu-based bulk metallic glasses

K. Tao, J. C. Qiao, L. Zhang, J. M. Pelletier

Dynamic mechanical response of ZrCu-based bulk metallic glasses

K. Tao [a], J.C. Qiao [a,b,*], L. Zhang [c], J.M. Pelletier [d,*]

[a] *School of Mechanics, Civil Engineering and Architecture, Northwestern Polytechnical University, Xi'an 710072, China*

[b] *Chongqing Science and Technology Innovation Center of NPU, Chongqing 401135, China*

[c] *Shi-changxu Innovation Center for Advanced Materials, Institute of Metal Research, Chinese Academy of Sciences, Shenyang 110016, China*

[d] *Université de Lyon, MATEIS, UMR CNRS5510, Bat. B. Pascal, INSA-Lyon, F-69621 Villeurbanne Cedex, France*

* Corresponding author:
E-mail address: qjczy@nwpu.edu.cn (Professor Dr. J.C. Qiao)
jean-marc.pelletier@insa-lyon.fr (Professor Dr. J.M. Pelletier)

Abstract

The thermal stability and the dynamic mechanical relaxation behavior of $(Zr_{50}Cu_{40}Al_{10})_{100-x}Dy_x$ (at.%) (x=0 or 2) metallic glasses were investigated by differential scanning calorimetry (DSC) and dynamic mechanical analysis (DMA). In the case of the $(Zr_{50}Cu_{40}Al_{10})_{100-x}Dy_x$ (x=0 or 2) metallic glasses, atomic mobility increases by introduction of the Dy element. The activation energy of the the main α relaxation process and fragility index were discussed according to the DMA measurements. With the help of the time-temperature superposition (TTS) principle, the master curves of the model alloys were established, the Kohlrausch-Williams-Watts (KWW) function and quasi-point defects (QPD) theory were used to descirbe the master curves of the metallic glasses. The characteristic parameters related to microstructural heterogeneity in the KWW equation and the QPD model, Kohlrausch exponent β_{KWW} and the correlation factor χ were evaluated. In parallel, the elastic, viscoelastic and viscoplastic responses of the model alloys have been analyzed based on the DMA results. Our investigations demonstrated that introduction of the Dy increases the structure heterogeneity of the $(Zr_{50}Cu_{40}Al_{10})_{100-x}Dy_x$ (x=0 or 2) glassy system, which plays an important role in tailoring the dynamic relaxation behavior and mechanical properties of the metallic glasses.

Keywords: Metallic glass; Mechanical relaxation process; Microstructure heterogeneity; Quasi-point theory; Physical aging

1. Introduction

As a new class of metallic materials, metallic glasses (MGs) are well accepted to have potential for wide application as engineering and functional mateirals due to their unique physical/mechanical properties, such as the high strength and large elastic limit [1-8]. The physical properties of MGs strongly depending on its internal structural state at atomic level. It is well accepted that the metallic glasses are often stay in out of equilibrium (more disorderly) and always evolve very slowly to a more equilibrimum state (more orderly) at ambient temperature in a rugged and tortuous

energy landscape due to the random long range atomic structure [9-11]. Compared with the traditional metallic alloys, metallic glasses are absence of defects in metals, i.e. voids, dislocations as well as grain boundaries. How to establish the correlation between the "defects" and mechanical/physical properties is one of challenging issues of metallic glasses [12, 13]. Many experiments and simulations have demonstrated that metallic glasses are heterogeneous structure at micro-nano scale regions [2, 14-16]. Typically, the microstructure of the metallic glasses can be regarded as liquid-like region and solid-like region [17-19]. Mechanical and physical properties of metallic glass were inherited from the supercooled glass-forming liquid. Especially, it is well documented that dynamic mechanical relaxation behavior is a key topic to understand the the structural heterogeneity of metallic glasses [20, 21].

Dynamic mechanical analysis (DMA) (also called mechanical spectrocopy) is an powerful technique to obtian the informations on the atomic or molecular movements of glassy materials during the deformation process under a sinusoidal stress [22, 23]. According to the amplitudes of the stress, strain and phase lag, one can obtain some fundamental parameters, such as storage modulus, loss modulus and internal friction factor, et al. [24-26]. Benefitting from the advantages, DMA was widely used to probe the α and β relaxation processes of the galssy solids. Importantly, as proposed by Johari and Goldstein, the dynamic behaviour of metallic glasses is characterized by two phenomenons: (i) JG relaxation or β relaxation process, which is linked to the local movement of the atoms/molecules. The β relaxiaton is areversible process, and (ii) the mian α relaxation, which is related to large scale irreversible arrangement of atoms or molecules [27]. The dynamic relaxation modes provide an important route to probe "defects" and to understand the corresponding the relation between structure and property of metallic glass [12, 13]. Additionally, the glass main α relaxation process corresponds to the dynamic glass transition phenomenon [5, 28]. It should be stressed that β relaxation process is the main relaxation mode of the glassy solids. [29]. It has been proposed that the β relaxation should be explained by the translational motion of atoms localized in loosely packed regions. This description certainly assumes that β relaxation intrinsically correlates with and structurally

originates from structural heterogeneity of metallic glasses [18, 19, 30].

Potential energy landscape (PEL) theory proposed by Debenedetti and Stillinger, the β relaxation behavior has been interpreted as stochastically activated hopping events through "subbasins", while the α relaxation corresponds to the irreversible hopping across various landscape megabasins [31]. As initiallly proposed by Argon the deformation of MGs results from the cooperative shear motion of local arrangements involving tens of hundred atoms, namely shear transformation zones (STZs) [32, 33]. In addition, it has been observed that the activation energy of the β relaxation is nearly the same as the potential energy barriers of STZs [34]. Therefore, the dynamic relaxation behavior is intrinsic linked to the deformation mechanism of glassy solids. Johnson and Samwer proposed that isolated events of the STZs confined within the elastic matrix are linked to the β relaxation process, while percolation of these STZs leads to the collapse of the confining matrix and breakdown of elasticity are associated with the α relaxation [10, 35]. Therefore, understanding of dynamic relaxation behavior is important issue for probing the nature of metallic glass, microscopic structural heterogeneity, physical aging, deformation mechanism and the mechanical properties. It is well known that physical properties of these dynamic relaxation modes depend on the chemical composition of the metallic glasses. According to previous researches, micro-alloying is an effective way to tune the mechanical behavior and relaxation process [25, 36-40]. For instance, Yu et al. reported that the intensity of β relaxation is suppressed by the introduction of aluminum in a $Cu_{45}Zr_{45}Al_{10}$ metallic glasses [29]. The relaxation behavior of ZrCu-based metallic glasses can also be modified by introducing hydrogen: α and β relaxation shift to higher temperature region with a lower intensity, and a β′ relaxation occurs with relative higher intensity [38]. These samples with minor addition of hydrogen element exhibit a higher density of "soft spots" , which promotes the nucleation and occurence of multiple shear bands. As a consequence, plasticity of the metallic glasses could be ameliorated. It is widely known that "soft spots" of the metallic glasses correspond to the loose-packed zones, which are easily to initiate local arrangements. Previous literatures have pointed out that β relaxation

process is connected with these loose-paked zones [2, 41, 42]. Furthermore, it has been demonstrated that by the addition of Dysprosium (Dy) of $(Zr_{50}Cu_{40}Al_{10})_{98}Dy_2$ glassy system, the β relaxation process becomes more evident and the compressive plasticity is enhanced to some extend, which is ascribed to the improvement of concentration of the "defects" of metallic glasses [25].

Many theoretical models have been developed to probe the deformation mechanism and physical properties of amorphous materials i.e. free volume therory [43-45], flow units model [46, 47] as well as interstitialcy theory [48, 49]. Free volume is defined as the excess volume compared to an ideal disordered atomic configuration of maximum density. Different from the free volume model, the interstitialcy theory was originally proposed by Granato [48, 49]. It is widely accepted that interstitials reside in a split configuration and sharing a lattice site with another atom. In addition, flow units can be regarded as nanoscale regions which correspond to pseudo "defects" in metallic glasses [21, 47]. Unlike the elastic matrix, the nanoscale flow units show lower elastic moduli, higher energy state and lower hardness. In parallel, Perez et al. assumed that the glass structure consists of packed atoms with regions of enthalpy or entropy fluctuations [50-52]. These regions are called quasi point defects (QPD). Compared to the crystals, a lower density region can be seen as a vacancy, while a higher density region is comparable to an interstial. The QPD determine the atomic or molecular mobility through hierachically correlated atoms arrangements. The QPD theory refers to a conceptual scenario for the atomic rearrangements occuring in favoured sites (defects) that are rich of free volume and responsible for the non-elastic deformation. These movements can be dissociated in anelastic (reversible) and viscoplastic (permanent) contribution [53]. Focusing on the oxidy glass and amorphous polymers, tremendous researches have been devoted to the non-linear mechanical response to mechanical loading [22, 53, 54]. In principle, their non-linear mechanical response is associated with the processes characterized by a strong dependence on the temperature, strain rate and the intrinsic internal heterogeneous atomic structure [19, 22, 54]. Therefore, modelling approaches are needed to describe the feature behavior in order to allow us to predict or design the

function of metallic glass under the current circumstance of poor plasticity.

Micro-alloying is an important way to tune the mechancial properties of the metallic glasses [25, 38, 39]. Furthermore, it has been demonstrated that by the addition of dysprosium (Dy) of $Cu_{46}Zr_{43}Al_7Dy_4$ glassy system, the β relaxation process becomes more evident and the compressive plasticity was enhanced to some extend, which is ascribed to the improvement of concentration of the "defects" of metallic glasses [25]. In the present study, the dynamic mechanical relaxation processes of $(Zr_{50}Cu_{40}Al_{10})_{100-x}Dy_x$ (x=0 or 2) metallic glasses were investigated by DMA. In the framework of the QPD theory, dynamic mechancial behavior of the model alloys were described. The experiemntal results suggested that introduction of the Dy increases the structure heterogeneity of the $(Zr_{50}Cu_{40}Al_{10})_{100-x}Dy_x$ (x=0 or 2) metallic glasses. It should be emphasized that micro-alloying is an important technique to tailor the dynamic relaxation modes of metallic glasses.

2. Experiment procedure

The samples with nominal composition $(Zr_{50}Cu_{40}Al_{10})_{100-x}Dy_x$ (x=0 or 2) were prepared by the arc-melting technique. Master-alloy ingots were first prepared using a mixture of high purity (99.99%) Zr, Cu, Al and Dy elements in an argon atmosphere. The master alloy was re-melted at least five times to ensure the chemical homogemeity of the model alloys. Metallic glass plates with a thickness of 2 mm were prepared by copper mould casting technique.

X-ray diffraction (XRD) was conducted to confirm the glassy nature by Cu Kα radiation produced by a Bruker D8 advance X-ray diffractometer at room temperature. The specimens were checked by Transmission electron microscopy (TEM, FEI Titan G3) with probe and image Cs correctors. TEM specimens were cut from the samples and ion milled using a Gatan 695 device. Differential scanning calorimetry (DSC) experiments were performed through a commercial instrument (DSC, PerkinElmer) at a heating rate of 10 K/min in a high purity dry nitrogen atmosphere. The glass transition temperature and the onset crystallization temperature were determined based on the DSC curve.

Plate samples were cut with approximate dimensions 30 (length) × 2.0 (width) × 1.0 mm (thickness) by an electric discharge machine, then polished by 2000 grit SiC paper. Finally, the samples weresonicated in a methanol bath to remove surface contaminants. The dynamic relaxation behavior of metallic glasses was investigated using two different DMA devices, i.e. a commercial device (DMA, Q800, TA, USA) and a home-made inverted torsion instrument with a vacuum enviroment in INSA de Lyon [55]. The first one uses tensile stress, leading to the determination of the Young modulus (E), while in the second one a shear stress is applied and the shear modulus (G) is deduced. A periodic stress is applied $\sigma = \sigma_0 \sin(\omega t)$, where ω is the angular frequency. The complex modulus E^*, which can be defined as $E' + iE''$, and shear modulus, $G^* = G' + iG''$, can be deduced from σ/ε, where E' and G' are the storage modulus, E'' and G'' are the loss modulus. Conequently, the loss factor, also termed as internal friction, $\tan\delta = E''/E'$ or $\tan\delta = G''/G'$can be determined. It should be noted here that $\tan\delta$ is related to the energy loss per load cycle: $\tan\delta = 1/2\pi(\Delta W/W)$, where the energy loss ΔW is caused by the movement of atoms during relaxaion process. Two different kinds of experiments were performed: (i) Isochronal tests were conducted with a single cantilever mode at a heating rate of 3 K/min and a driving frequency of 1 Hz on the DMA Q800. (ii) Isothermal experiments were carried on the home-made inverted torsion instrument with various frequency from 0.01 to 2 Hz (the temperature interval is 5 K).

3. Experimental results and discussions

3.1 Structural and thermal properities of the $(Zr_{50}Cu_{40}Al_{10})_{100-x}Dy_x$ (x=0 or 2) metallic glasses

XRD were performed to check the amorphous nature of the $(Zr_{50}Cu_{40}Al_{10})_{100-x}Dy_x$ (x=0 or 2) (as-cast state) metallic glasses. As shown in **Fig.1 (a)**, the XRD patterns exhibit a broad maximum with no detectable crystalline Bragg peaks, which suggests that the model alloys are fullly amorphous.

The glass transition and crystallization events were determined by DSC, which is shown in **Fig.1 (b)**. In the case of the $Zr_{50}Cu_{40}Al_{10}$ and $(Zr_{50}Cu_{40}Al_{10})_{98}Dy_2$ bulk

metallic glasses, the glass transition temperature T_g is 691 K and 683 K, respectively. At the same time, the crystallization temperature of $Zr_{50}Cu_{40}Al_{10}$ and $(Zr_{50}Cu_{40}Al_{10})_{98}Dy_2$ is 763 K and 756 K, respectively. It is evident that T_g is decreased by the addition of Dy. In parallel, in good agreement with other Zr-based metallic glasses, the $(Zr_{50}Cu_{40}Al_{10})_{100-x}Dy_x$ (x=0 or 2) bulk metallic glasses show broad super-cooled liquid regions (SLRs) [24, 25]. In addition, as shown in **Fig.2**, the glassy structure was confirmed by the featureless TEM microstructures and the high-resolution TEM (HRTEM) images, of which the corresponding fast Fourier transformation (FFT) patterns only present a diffuse halo, further confirming that the amorphous structure of the model alloys in the current investigations. It should be emphasized that there is no formation of oxide inclusions in the introduction of the rare earth metals of $(Zr_{50}Cu_{40}Al_{10})_{100-x}Dy_x$ (x=0 or 2) bulk metallic glasses.

3.2 Dynamic mechanical analysis

3.2.1 Isochronal analysis

In order to probe the dynamic mechanical behavior of the $(Zr_{50}Cu_{40}Al_{10})_{100-x}Dy_x$ (x=0 or 2) metallic glasses, the samples were heated in the isochronal mode by DMA. **Fig.3 (a)** shows the normalized storage modulus E'/E_u and the normalized loss modulus E''/E_u of $(Zr_{50}Cu_{40}Al_{10})_{98}Dy_2$ metallic glass. Herein, it should be stressed that E_u is the unrelaxed modulus at the room temperature, which is assumed as the value of the storage modulus at ambient temperature. Evidently, compared with the storage modulus, the contribution of loss modulus during the deformation process at the ambient temperature could be neglected. There are three tempeature regions can be observed based on the temperature-heating process of the model alloy (as shown in **Fig.3 (a)**), which is simiar to other typical metallic glasses [25, 56]. (I) When the temperature below 630 K, the normalized storage modulus E' is high and nearly remains constant, while the normailzed loss moduls around zero. It suggests that the elastic deformation dominate the deformation process in this temperature domain. As we mentioned in the Introduction section, unlike the La-based metallic glasses [26], there is no pronounced β relaxation peak was observed of the ZrCu-based metallic

glass. (II) When the temperature ranges from 630 K to 740 K, it can be seend that the storage modulus E' decreases drastically. On the other hand, the loss modulus E'' increases, which reaches the maximum value around 725 K, which corresponds to the α relaxation of glassy materials. Generally speaking, the α relaxation process of glasses, which is closely associated with the the cooperative movements of the atoms or molecules [23, 25]. (III) When the temperature above 740 K, it is found that the storage modulus E' and the loss modulus E'' increase sharply, which corresponds to the precipitation of the crystalline phases.

In parallel, dynamic mechanical relaxation processes of metallic glasses is very sensitive to the driving frequency. **Fig.3 (b)** shows the normalized loss modulus of $(Zr_{50}Cu_{40}Al_{10})_{98}Dy_2$ metallic glass *versus* the temperature at different frequencies (1, 2, 4 and 8 Hz) with a constant heating rate of 3 K/min. The α relaxation peak shifts to a higher temperature by increasing the driving frequency. The activation energy can be deduced from the correlation between the driving frequency and the characteristic temperature by the Arrhenius equation [52]:

$$f = f_0 exp\left(-\frac{E_\alpha}{k_B T_p}\right) \quad (1)$$

where f is the driving frequency, f_0 is a pre-exponential factor, E_α is the activation energy of the main α relaxation and T_α is the characteristic temperature of α relaxation. As a consequence, the activation energy of the $Zr_{50}Cu_{40}Al_{10}$ and $(Zr_{50}Cu_{40}Al_{10})_{98}Dy_2$ metallic glasses is 5.73 eV and 5.57 eV, respectively. The results in the current research are in good agreement with the other typical ZrCu-based metallic glasses [56, 57].

In the case of metallic glasses, the dynamic relaxation behavior is closely linked to the fragility parameter [58]. Angell proposed the kinetic fragility m, which is connected to the slow down of glass transition dynamics and proposed to characterize the deviation from the Arrhenius relationship in the characteristic relaxation time *versus* temperature curve [12, 59]. It is accepted that the concept of fragility has been used to classify the viscosity or the relaxation time of glass forming liquid with temperature approaching the glass transition temperature T_g, and can be defined by

[59, 60]:

$$m = \mathrm{d}\log_{10}\tau_\alpha/\mathrm{d}\left(T_g/T\right) = E_\alpha/(RT_g \ln 10) \quad (2)$$

From the m value we can learn how fast the viscosity decreases near the glass transition temperature T_g [59]. Typically, the fragility parameter m of the glassy materials ranges from 16 to 200 [59]. In the current study, the fragility parameter m is = 41 for $Zr_{50}Cu_{40}Al_{10}$ metallic glass. Compared with other metallic glasses, four fragile metallic glass formers were chosen: $Zr_{41.2}Ti_{13.8}Cu_{12.5}Ni_{10}Be_{22.5}$ (m=50), $La_{60}Ni_{15}Al_{25}$ (m=51), $Al_{88}Y_7Fe_5$ (m=55) and $Gd_{55}Co_{25}Al_{20}$ (m=74) [9]. It indicates that the current ZrCu-based metallic glass is a stronger glassy system due to the value of fragility parameter m is lower. We will discuss the inforamtion of fragility of glassy solids in the next section. Therefore, following the criteria defined in the reference [50], it is reasonable to believe that ZrCu-based metallic glasses have a dense-packed structure and a high glass-forming ability.

The temperature dependence of the normalized loss modulus E''/E_u for the $(Zr_{50}Cu_{40}Al_{10})_{100-x}Dy_x$ (x=0 or 2) metallic glasses is shown in **Fig.4**. The peak temperature of the normilized loss modulus moves to the lower temperature by the addition of Dy, which is in accordance with the results of glass transition temperature obtained by DSC (which was shown in **Fig.1 (b)**).

It should be noted that the JG relaxation is not clearly observed at the low temperature region [25, 40] (**Fig. 4).** However, there is only broad hump (sometimes referred as excess wings) can be observed around 560-650 K and 575-660 K for $Zr_{50}Cu_{40}Al_{10}$ and $(Zr_{50}Cu_{40}Al_{10})_{98}Dy_2$ bulk metallic glasses, respectively [58]. These humps may be considered as large and diffuse JG relaxations (Excess wing). The magnitude of the excess wing is increased by increasing the Dy content. The influence of micro-alloying on the JG relaxation in the $(Zr_{50}Cu_{40}Al_{10})_{100-x}Dy_x$ (x=0 or 2) glassy system needs to be addressed from a perspective of mixing enthalpy in metallic glass systems. The JG relaxation is linked to dynamic heterogeneity in metallic glasses, especially a local diffusion in loose-packed isolated regions which are often refered as defects and flow units [9, 18, 23]. The mixing enthalpy of Zr-Cu, Zr-Al, Zr-Dy are

-23, -44 and 8 kJ/mol, while the mixing enthalpy of Cu-Al, Cu-Dy and Al-Dy are -1, -22 and -38 kJ/mol, respectively [61, 62]. According to the emprical rules to determine ΔH_{mix}, the mixing enthalpy of the $(Zr_{50}Cu_{40}Al_{10})_{100-x}Dy_x$ (x=0 or 2) metallic glasses is -30.88 (x=0) and -31.55 (x=2), respectively. Therefore, the addition of Dy decreases the mixing enthalpy, which explains the increase in the intensity of the β relaxation, or at least the value of the loss modulus at low temperature. Similar conclusions have been obtained in previous studies [25, 29]. In addition, the peak of the loss factor moves to lower temperature, which agrees with the phenomena observed on the DSC curve, moving to lower temperature in **Fig.1 (b)**.

Perez and his coworkers proposed the quasi-point defect theory, which can be used to describe the mechanical properties of amorphous materials with respect to its microstructure [51, 52, 63, 64]. The atomic rearrangement will preferentially occur at these defect sites, whether in the process of thermal activation or stress activation. **Fig.5 (a)** shows a symbolic scheme of an amorphous solids withthe associated defect sites. The effect of a mechanical stimulus such as a shear stress is applied. At the first stage of the deformation, these sites are thermomechanical activated under the mechanical stimuls(as seen in **Fig.5 (b)**), which bring the localized elementary motions of several atoms or molecules, preferentially oriented along the maxmium shear plane. It should be noted that these atomic rearrangements are responsible to the second β relaxation process of amorphous solids [29]. The nucleation and growth from these sheared micro domains are responsible to the onset of the inelastic response of the glassy materials (as shown in **Fig.5 (c)**). When the applied stress is long enough, new sheared micro domains are nucleated (as seen in **Fig.5 (d)**), whichcauses plastic deformation by the coalescence of shear micro domains. The dynamic relaxation behavior is generally related to atomic or molecular motions and the relaxation time is temperature dependence. As described in earlier reports [65, 66], the hierarchically correlation of dynamic relaxation leads to the following expression for the mean time τ_{mol}, which characterizes the atomic mobility as:

$$\tau_{mol} = t_0 \left(\frac{\tau_\beta}{t_0}\right)^{1/\chi} \quad (3)$$

where τ_{mol} corresponds to the mean duration of the movement of a structural unit over distance equal to its dimension. τ_β is the mean time of the thermally activated jump of structural units and follows an Arrhenius law:

$$\tau_\beta = \tau_{0\beta} \exp\left(\frac{U_\beta}{kT}\right) \quad (4)$$

where U_β is the apparent activation energy for the movements of structural units and is then related to the β relaxation mode of glassy solids. t_0 is a scaling factor and χ is a correlation factor range from 0 to 1:

(I) $\chi = 0$: any movement of a structural units requires the motion of all other units (maximum order, corresponding to a perfect crystal).

(II) $\chi = 1$: all the movements are independent on each other (maximum disorder, corresponding to a perfect gas). Should note that, **Eq.(4)** only express the thermal activation process, so it can be modified to characterize the mechanical activation [65]:

$$\tau_\beta = \tau_{0\beta} \exp\left(\frac{(U_\beta + \Omega p)\left(1 - \frac{\sigma_{max}}{\sigma_0}\right)^{3/2}}{kT}\right) \quad (5)$$

where p is the hydrostatic pressure, Ω is the shear stress which enables the energy cross-over at 0 K. σ_{max} is the activation shear stress or the maximum shear stress.

Because the correlation parameters are connected to the disordered state, it is reasonable to be related to the microstructure evolution. If one neglects the aging effect and without any external stimulus, the disorder is assumed constant in a "frozen" glass state, whereas it increases linearly with temperature when the temperature rises to the glass transition temperature T_g. In addition, taking the scenario proposed for atoms rearrangements under an external mechanical stimulus, the disorder parameter must be related to the state of non-elastic strain within the sample. Besides, an increase of the anelastic c©©omponent corresponds to an increase of the number/size of QPD, i.e., an increase of the disorder. However, the viscoplastic process may provoke the decrease of the disorder due to it leads to the larger scale atomic rearrangements. So, in a frozen or iso-configurational state, χ has a constant value, while in a metastable thermodynamic equilibrium, χ increases with the temperature

T. The variation of the correlation factor χ with the temperature can be expressed by [67]:

$$\chi(T,\gamma) = \chi(\mathrm{T}) + a_{ve}\gamma_{ve} - a_{vp}\gamma_{vp} \tag{6-1}$$

$$\chi(T) = \chi(T_g),\ T < T_g \tag{6-2}$$

$$\chi(T) = \chi(T_g) + a(T - T_g),\ T > T_g \tag{6-3}$$

where a_{ve}, a_{vp} and a depend on the material.

The atomic mobility is assisted by the microscopic structure heterogeneity in metallic glass, from the point of the potential energy landscape theory, i.e., nanoscale fluctuations of the entropy or enthalpy. These fluctuations can be described as quasi-point defects (QPD), Their concentration C_d is temperature dependence and can be evaluated from the Boltzmann statistics [51]:

$$C_d = \left(1 + \exp\left(-\frac{\Delta S_F}{k}\right)\exp\left(\frac{\Delta H_F}{kT}\right)\right)^{-1} \tag{7}$$

where ΔS_F and ΔH_F is the function entropy and enthalpy of a QPD, respectively.

According to the concepts mentioned above, the compliance $J(t)$ is the combination of elastic, anelastic and viscoplastic components of the deformation. In amorphous solids, $J(t)$ can be described as [54]:

$$J(t) = \frac{1}{G_{el}} + A\left\{1 - \exp\left[-\left(\frac{t}{\tau_{mol}}\right)^{\chi}\right]\right\} + A'\left(\frac{t}{\tau_{mol}}\right) \tag{8}$$

where G_{el} is the elastic modulus at infinite frequency, A and A' are parameters proportional to quasi-point concentration C_d, thus, also proportional to the anelastic component of the deformation. The description of the dynamic modulus and the frequency can be simply given by the Fourier transform of **Eq.8**, and considering the residual component of the modulus, i.e., $G_r = G(\infty)$:

$$G^*(i\omega) = G_r + \frac{G_{el} - G_r}{1 + \eta(i\omega\tau_{mol})^{-\chi} + (i\omega\tau_{mol})^{-1}} \tag{9}$$

where G_u is the unrelaxed modulus, η is a numerical factor, near unity, but depending on C_d, ω is the angular frequency.

Furthermore, Perez et al. [64] have given the expression of the internal friction $\tan\ \delta = G''/G'$:

$$\ln(\tan\ \delta) = \frac{U_\beta}{kT} - \chi\ln\omega - \chi\ln\tau^* + \ln\eta \tag{10}$$

with:

$$\tau^* = t_0 \left(\frac{\tau_{0\beta}}{t_0}\right)^{1/\chi} \quad (11)$$

When the temperature below the glass transition temperature T_g, the material is in an iso-configurational state and χ is constant. On the other hand, when the temperature above the glass transition temperature T_g the concentration of defect increases due to a faster diffusion, and therefore χ increases. Consequently, one can plots $\ln(\tan\ \delta)$ *versus* the reciprocal of the temperature $1/T$ at a fixed frequency and then get the value of U_β. In a similar method, χ can be deduced from the plot of $\ln(\tan\ \delta)$ *versus* $\ln(\omega)$ at a fixed temperature.

Fig.6 shows the logarithm of internal friction $\ln(\tan\ \delta)$ *versus* the reciprocal of the temperature $1/T$ for the $(Zr_{50}Cu_{40}Al_{10})_{100-x}Dy_x$ (x=0 or 2) bulk metallic glasses. Such a plot can be used to determine the glass transition temeprature T_g and crystalline temperature T_x. In fact, the aforementioned theory has been successfully used by previous researches to analyze viscoelasticity and viscoplasticity behavior in Zr- and Pd-based bulk metallic glasses [68, 69]. The characterisic parameters for both alloys obtained from mechanical spectroscopy analysis based upon the physical model are summarized in the **Table 1**.

Table1 The characteristic parameters determined by mechanical spectroscopy analysis

Metallic glasses	T_g (K)	T_x (K)	T_x-T_g (K)	$U\beta$ (eV)
$Zr_{50}Cu_{40}Al_{10}$	693	752	59	0.628
$(Zr_{50}Cu_{40}Al_{10})_{98}Dy_2$	681	738	57	0.578

As shown in **Table 1**, glass transition temperature T_g, temperature corresponding to the onset of crystallization T_x and the range of super-cooled liquid $\Delta T_x = T_x - T_g$ decrease with Dy element addition, which is consistent with the results of calorimetric analysis. It should be noted that the values of the characteristic temperatures deduced from the dynamic mechanical spectroscopy analysis are very close to that obtained through the DSC curves. It can be clearly seen that the activation energy U_β, which is the height of the energy barrier for the elementary movement related to the β

relaxation for the $Zr_{50}Cu_{40}Al_{10}$ and the $(Zr_{50}Cu_{40}Al_{10})_{98}Dy_2$ metallic glasses is 0.628 and 0.578 eV, respectively. The experimental results demonstrates that the addition of Dy element enhances the atomic mobility, thus decreases the mean time τ_β and the relaxation time of related β relaxation. Based on the cooperative shear model, the activation erergy E_β is equivalent to the potential energy barrier for operating of STZs, a lower activation energy E_β linking to a compliant matrix confinement [10, 70, 71]. Besides, the β relaxation closely relates to the plasticity in metallic glass, which is believed as a thermal-driven percolation process of STZs [34]. It is reported that the STZs prefer to nucleating in the liquid like region [29, 72]. Thus, we can assumed that the lower the activation energy, the more the STZs could be triggered. This in turn will promote the nucleation and propagation of shear bands and potentially improve the plasticity in metallic glasses [38].

3.2.2 Physical aging of metallic glass

Kinetics of the structural relaxation in $(Zr_{50}Cu_{40}Al_{10})_{98}Dy_2$ bulk metallic glass was investigated by performing isothermal DMA measurements with a driving frequency of 1 Hz. **Fig.7** (blue line) shows the loss factor $\tan\delta$ evolution *versus* annealing time at 625 K in the $(Zr_{50}Cu_{40}Al_{10})_{98}Dy_2$ bulk metallic glass. The loss factor $\tan\delta$ decreases sharply with the annealing time, while the storage modulus E' increases slightly.

Dynamic mechanical relaxation process in amorphous materials presents non-exponential, non-Arrhenius and nonlinear characteristics. It is believed that physical aging below the glass transition temperature can tune the physical and mechanical behaviors of glassy materials [24, 73, 74]. From the perspective of the kinetics, the Kohlrausch-Williams-Watts (KWW) equation was widely used to describe the kinetics of physical aging of amorphous materials based on DSC experimental results as well as DMA experiments [12, 13, 56]. The KWW function is defined as follows [75]:

$$\tan\ \delta(t=0) - \tan\ \delta(t) = A\left\{1 - \exp\left[-(t_a/\tau)^{\beta_{aging}}\right]\right\} \quad (12)$$

where $A = \tan\ \delta(t) - \tan\ \delta\ \ (t \to \infty)$ is the maximum magnitude of the relaxation. t_a stands for the aging time, τ is characteristic relaxation time and β_{aging} is the Kohlrausch exponent, which ranges from 0 to 1, which is related to the dynamic inhomogeneity [47].

The solid lines in **Fig.6** represents the fitted curve using **Eq. (12)**. The Kohlrausch exponent β_{aging} is around 0.50 when the physical aging temperature is close to the glass transition temperature T_g of $(Zr_{50}Cu_{40}Al_{10})_{98}Dy_2$ metallic glass, which is in accordance with previous reported experimental results [24].

The annealed sample has been reheated after the process of physical aging. The inset of **Fig.8 (b)** shows the schematic illustration of the temperature history during the *in-situ* heating process. As shown in **Fig.8 (a)**, the storage modulus of annealed sample is higher than that of the as-cast state. But there is an interesting phenomenon in **Fig.8 (b)**, an evident peak which is like the β relaxation process can be noticed in the annealed metallic glasses [29, 40]. We speculate that it could be due to phase separation during the physical aging process. However, a more detailed scrutinize is required, and it will be reported in the other work. **Fig.9** is the HRTEM image of the annealed sample of $(Zr_{50}Cu_{40}Al_{10})_{98}Dy_2$ metallic glass. It is evident that there is no formation of nucleation or crystalline phase during the physical aging process of the model alloy. As we discussed in the previous section, it should be noted that the glassy materials are in a non-equilibrium state below the glass transition temperature T_g. For metallic glasses or other amorphous materials, when the annealing temperature T_a is below T_g, the structure of the glassy materials tends towards more stable state [4]. As shown in **Fig.10**, the difference in specific heat capacity, Δc_p, induced by physical aging and as-cast state of $(Zr_{50}Cu_{40}Al_{10})_{98}Dy_2$ metallic glass. It should be emphasized that the as-cast state shows a noticeable signal of relaxation enthalpy $\Delta H = (1.61 \pm 0.06)$ kJ mol^{-1} near T_g, which indicating that the specimen has certain free volume content after suction mold casting. It is reported that the sub-T_g physical aging of glassy materials is accompanied by reduction of free volume, which is closely connected with topological short-range ordering and chemical

short-range ordering [76]. The decrease of the free volume is accompanied by a decrease of the enthalpy of the metallic glass. As a consequence, isothermal annealing below the glass transition temperature leads to a reduction of the free volume up to $\Delta H = (0.35 \pm 0.04)$ kJ mol^{-1}. Besides, noted that, an increase of the endothermic effect can be observed, which is ascribed to more free volume generation takes place in a relaxed specimen [76].

3.2.3 Isothermal frequency scanning analysis

In order to further study the dynamic mechanical relaxation behavior, isothermal frequency scanning experiments were carried out in the $(Zr_{50}Cu_{40}Al_{10})_{100-x}Dy_x$ (x=0 or 2) metallic glasses (as shown in **Fig.11**). The experimental results could be summarized as follows: (i) At the lower frequency, the storage modulus G' is low. (ii) The loss modulus G'' shows a peak corresponding to the α relaxation at high temperature, and it shifts toward to a lower frequency when temperature decreases. (iii) There is no evident JG relaxation behavior according to the loss modulus.

From the prespective of the frequency window, the pronounced peaks wereobserved at high temperature, which corresponds to the main α relaxation of metallic glasses. This is in line with the results obtained in **Fig.3 (a)**. The characteristic time of the α relaxation τ_α of metallic glass can be obtained from the general relation: $2\pi f \tau_\alpha = 1$.

On the basis of the time-temperature superposition (TTS) principle, master curve may be plotted with a reference temperature. The initial curves are shifted by the frequency shift factor a_T [77, 78]:

$$\ln a_T = \ln\tau - \ln\tau_r \tag{13}$$

where τ and τ_r are the relaxation times at temperatures T and the reference temperature T_r, respectively. The variation of the relaxation time τ with temperature may be described using the following equation [78]:

$$\ln a_T = \frac{E_\alpha}{R}\left(\frac{1}{T} - \frac{1}{T_r}\right) \tag{14}$$

where R is the gas constant and E_α is the activation erengy of the α relaxation.

Fig.12 shows the master curves of $(Zr_{50}Cu_{40}Al_{10})_{100-x}Dy_x$ (x=0 or 2) metallic

glasses. As proposed by Williams et al., the Kohlrausch-Williams-Watts (KWW) relaxation relation can be used to well describe the α relaxation process of the loss modulus spectra of glassy solids [79]:

$$G''(\omega) = \Delta G_\alpha L_{i\omega}\left[-\frac{d\varphi_\alpha(t,\tau_\alpha)}{dt}\right] \quad (15)$$

With:

$$\varphi_\alpha(t,\tau_\alpha) = \exp\left[-(t/\tau_\alpha)^{\beta_{\mathrm{KWW}}}\right] \quad (16)$$

where ΔG_α is the relaxation strength, which is equal to the difference between the unrelaxed modulus G_u and the well relaxed modulus G_r. $L_{i\omega}$ indicates the Laplace tranform, and β_{KWW} stands for the Kohlrausch exponent, which ranges from 0 to 1 and can be obtained from the isothermal spectra.

Based on the previous investigations, Bergman derived a relaxation equation, which can be used to the main relaxation process of the amorphous materials (i.e. metallic glasses as well as amorphous polymers) [80]:

$$G'' = G_p / \left\{1 - \beta_{\mathrm{KWW}} + \frac{\beta_{\mathrm{KWW}}}{1+\beta_{\mathrm{KWW}}}\left[\beta_{\mathrm{KWW}}\left(\omega_p/\omega\right) + \left(\omega/\omega_p\right)^{\beta_{\mathrm{KWW}}}\right]\right\} \quad (17)$$

where G_p is the normalized loss modulus and ω_p indicates the peak frequency.

As shown in **Fig.12 (a)**, the master curves of $(Zr_{50}Cu_{40}Al_{10})_{100-x}Dy_x$ (x=0 or 2) metallic glasses can be well described by **Eq.(17)**. The value of β_{KWW} in $Zr_{50}Cu_{40}Al_{10}$ and $(Zr_{50}Cu_{40}Al_{10})_{98}Dy_2$ metallic glasses is 0.49 and 0.48, respectively, which indicates a slight increase of dynamic heterogeneity by introducing the element Dy. **Fig.12 (b)** displays the master curves fitted by **Eq.(9)** in the QPD model. The correlation factor χ values of $Zr_{50}Cu_{40}Al_{10}$ and $(Zr_{50}Cu_{40}Al_{10})_{98}Dy_2$ metallic glasses is 0.334 and 0.381, respectively. The results demonstrated that the increase of dynamic heterogeneity induced by introducing the Dy element, which is in good accordance with the discussion in the previous section.

The shift factor a_T *versus* various isothermal temperature for $(Zr_{50}Cu_{40}Al_{10})_{98}Dy_2$ metallic glasses is presented in **Fig.13**. According to the **Eq.(17)**, the apparent activation of α relaxation can be obtained. When the temperature increases, the viscosity increases sharply in the glass system, and the activation energy E_α is 6.08 and 5.96 eV for $Zr_{50}Cu_{40}Al_{10}$ and $(Zr_{50}Cu_{40}Al_{10})_{98}Dy_2$, respectively.

Noted that the activation energy E_α calculated here are nearly equal to the values obtained in the previous section, this indicates that the activation energy of α relaxation is an intrincically properties which does not change with the testing driven frequency.

As we mentioned in the previous section, the correlation factor χ can be determined by a plot of $\ln(\tan\delta)$ *versus* $\ln(\omega)$. As shown in **Fig.14**, all the experimental results could be well described by the QPD model. It should be mentioned that the correlation factor χ remains constant below the glass transition temperature T_g, which is consistently with the prediction of QPD model. Based on the QPD model, the microstructure of the glass materials is staying in an iso-configuration state when the temperature below T_g. It implied that the concentration of the "defects" concentration of glassy materialsis nearly constant. When the temperature surpasses the glass transition temperature T_g, the glassy materials are no longer stay in an iso-configuration state. Consequently, the correlation factor χ increases as a function of temperature. By increasing the temperature, the atomic diffusion is accelerated in the case of metallic glasses or molecules. It is expected that the correlation factor χ provides an indiactor of short-range order as well as the concentration of the quasi-point defects, which reflects the atomic or molecular mobility in glassy solids [18, 25, 33].

Specifically, it is interesting to note that the parameter *a* in the **Eq.(6-3)**, which indicates the slope of the curve $\ln(\tau)$ *versus* $1/T$ just above the glass transition temperature T_g and the fragility parameter m for the metallic glass system but is independent of the experimental condition (in opposition to the parameter m) [67, 81]. It can be seen that the value of the parameter *a* is 3.1×10^{-3} K^{-1} and 3.8×10^{-3} K^{-1} for $Zr_{50}Cu_{40}Al_{10}$ and $(Zr_{50}Cu_{40}Al_{10})_{98}Dy_2$ metallic glasses, respectively. Based on the linear fit of the correlation factor χ with the temperature above the T_g shown in **Fig.15**. The comparison between the prediction and experimental results of various glass forming systems is summarized in **Table 2**. It can be seen that the value of *a* of ZrCu-based metallic glass is intermediate between the reported oxidy glasses and polymers. Thus, it demonstrates that the fragility for ZrCu-based metallic glass is

intermediate, meanwhile, close to the fraglity of strong network glasses. It is in a good agreement with the fragility parameter m as mentioned in the previous section and the parameter a. As a consequence, the physical model could be used to succesfully describe the internal friction around the glass transition temperature in metallic glasses.

Table 2 Parameters of the typical glassy materials used in the physical model [67]

Type	Material	T_g (K)	U_β (eV)	$\chi(T_g)$	a ($\times 10^{-3}$ K^{-1})	Reference
Oxide	Silica	1493	-	0.47	-	[67]
	Silica-soda-lime	810	2.04	0.37	1	[67]
Metallic	$Zr_{50}Cu_{40}Al_{10}$	691	0.628	0.383	3.1	Current work
	$(Zr_{50}Cu_{40}Al_{10})_{98}Dy_2$	683	0.578	0.395	3.8	Current work
Polymeric	DGEBA-IPD	436	0.52	0.17	5.6	[67]
	PEEK	416	0.43/0.8	0.32	-	[67]
	PET	340	0.54	0.31	10	[67]
	PMABu	303	0.74	0.18	5	[67]
Molecular	Maltitol	310	0.61	0.34	5.3	[67]
	Sorbitol	268	0.61	0.32	5.8	[67]

3.2.3 Magnitude of the various components of the deformation

During the mechanical spectroscopy experiments of metallic glasses, three different components are involved in the mechanical response, i.e. elastic, viscoelastic and viscoplastic. With the set of consitutive equations recalled above, the QPD model allows a global describtion of the mechanical behaviour of an metallic glass from the linear to the non-linear range with account for the temperature, the loading conditions and the strain rate [53, 82]. Practically, this makes a strong correlations between the viscoelastic bahavior of the metallic glass characterized by the dynamic mechanical analysis. Rinaldi et al. gave the expression of the general compliance [53]:

$$J(t) = J_{el} + \Delta J_\beta \sum_i W_\beta^i \left(1 - e^{\left(-t/\tau_\beta^i\right)}\right) + \Delta J_{ve} \sum_i W_{el}^i \left(1 - e^{\left(-t/\tau_\beta^i\right)}\right) + \Delta J_{vp} \sum_i W_{vp}^i \left(1 - e^{\left(-t/\tau_\beta^i\right)}\right) \quad (18)$$

where J_{el} is the initial elastic compliance, taken as the inverse of the unrelaxed shear

modulus, W_β^i, W_{el}^i and W_{vp}^i are the relative weights of the Gumbel distribution law of the times τ_β^i, τ_{el}^i and τ_{vp}^i, respectively. Laplace-Carson transform of Eq.(18) directively gives the expression of the equivalent frequencial compliance J^* of the MGs:

$$J^*(\omega) = J_{el} + J_\beta \sum_i \frac{W_\beta^i}{1+i\omega\tau_\beta^i} + J_{ve} \sum_i \frac{W_{ve}^i}{1+i\omega\tau_{ve}^i} + J_{vp} \sum_i \frac{W_{vp}^i}{1+i\omega\tau_{vp}^i} \quad (19)$$

The real part of J^* is noted J' and the imaginary part J''. According to the previous research of Pelletier, the compliance can be deduced from the storage modulus and loss modulus (G' and G''): $J^* = J' - J'' = 1/G^* = 1/(G' + iG'') = J_{el} + J_{ve} + J_{vp}$ [22]. The imaginary parts is $J'' = -(J_{ve} + J_{vp})$.

Fig.16 (a) displays the evolution of J'' with the frequency. Both the low and high frequency sides tend toward a linear dependence with a slope of -0.8 and -1/3, respectively. Assuming a Newtonian flow, $J_{vp} = 1/\omega\eta$, the shear viscosity η can be expressed by: $\eta = G_u\tau_{mol}$, where G_u the unrelaxed is about 24 GPa. As shown in **Fig.12**, the characteristic time at T_g is $\tau_{mol} = 70$ s, so the shear viscosity η at this temperature is about 1.68×10^{12} Pa s. This is a reasonable value for the viscosity at T_g of metallic glasses. At the lower frequency, the visco-plasticity dominates the deformation process, this is because there is enough time for the atomic movements. By increasing of the frequency, visco-plasticity can not occur and the visco-elasticity becomes dominant. As proposed in a previous investigation [68], the elastic, visco-plastic and visco-plastic components over the whole frequency domain can be calculated as:

$$J_{el} = J' = \frac{G'}{G'^2 + G''^2} \quad (20\text{-}1)$$

$$J_{vp} = \frac{1}{\omega\eta} \quad (20\text{-}2)$$

$$J_{ve} = J'' - J_{vp} \quad (20\text{-}3)$$

The contribution of the elasticity, viscoelasticity and viscoplasticity during the deformation process of $Zr_{50}Cu_{40}Al_{10}$ metallic glass were shown in **Fig.16 (b)**. As discussed above, the viscous flow is the main contribution at lower frequency domain,

while the viscoelasticity dominate the deformation behavior at the higher frequency.

4. Conclusions

In conclusion, the dynamic mechanical relaxation behavior of $Zr_{50}Cu_{40}Al_{10}$ and $(Zr_{50}Cu_{40}Al_{10})_{98}Dy_2$ metallic glasses were investigated by DMA. Experimental results demonstrated that micro-alloying plays an important role in the dynamic mechanical behavior of the model alloys. Atomic mobility (i.e. concentration of the "quasi-point defects") increases by increasing the concent of Dy of $(Zr_{50}Cu_{40}Al_{10})_{100-x}Dy_x$ (x=0 or 2) glassy system. The quasi-point defects theory was used to describe the atomic mobility and dynamic mechanical behavior of the $(Zr_{50}Cu_{40}Al_{10})_{100-x}Dy_x$ (x=0 or 2) metallic glasses. The elastic, viscoelastic and viscoplastic response of the model alloy was analyzed based on the deformation process. The correlation parameter χ can be used to describe the concentration of the quasi-point defects, which is closely related to the microstructural heterogeneity of glassy solids. The experimental results of the ZrCu-based metallic glasses can be well described by the QPD theory. More importantly, our findings based on the dynamic mechanical behavior provides a route to understand the microstructural heterogeneity and physical properties of metallic glasses.

Acknowledgements

This work is supported by the National Natural Science Foundation of China (NSFC) (Grant Nos. 51971178 and 52171164), Natural Science Basic Research Plan for Distinguished Young Scholars in Shaanxi Province (Grant No. 2021JC-12) and the Natural Science Foundation of Chongqing (Grant No. cstc2020jcyj-jqX0001). The authors would like to thank H. Chen (Yanshan University) for providing the help of DSC experiments.

References:

[1] L.C. Zhang, Z. Jia, F. Lyu, S.X. Liang, J. Lu, A review of catalytic performance of metallic glasses in wastewater treatment: Recent progress and prospects, Prog. Mater. Sci. 105 (2019) 100576.

[2] J. Ding, S. Patinet, M.L. Falk, Y.Q. Cheng, E. Ma, Soft spots and their structural signature in a metallic glass, Proc. Natl. Acad. Sci. U.S.A. 111(39) (2014) 14052-14056.

[3] N. Li, J.J. Zhang, W. Xing, D. Ouyang, L. Liu, 3D printing of Fe-based bulk metallic glass composites with combined high strength and fracture toughness, Materials Design 143 (2018) 285-296.

[4] K. Tao, J.C. Qiao, Q.F. He, K.K. Song, Y. Yang, Revealing the structural heterogeneity of metallic glass: Mechanical spectroscopy and nanoindentation experiments, Int. J. Mech. Sci. 201 (2021) 106469.

[5] W.H. Wang, The elastic properties, elastic models and elastic perspectives of metallic glasses, Prog. Mater. Sci. 57(3) (2012) 487-656.

[6] X.Y. Wang, W.L. Dai, M. Zhang, P. Gong, N. Li, Thermoplastic micro-formability of TiZrHfNiCuBe high entropy metallic glass, J. Mater. Sci. Technol 34(11) (2018) 2006-2013.

[7] L. Ward, S.C. O'Keeffe, J. Stevick, G.R. Jelbert, M. Aykol, C. Wolverton, A machine learning approach for engineering bulk metallic glass alloys, Acta Metall. 159 (2018) 102-111.

[8] C.C. Yuan, F. Yang, X.K. Xi, C.L. Shi, D. Holland-Moritz, M.Z. Li, F. Hu, B.L. Shen, X.L. Wang, A. Meyer, Impact of hybridization on metallic-glass formation and design, Mater. Today 32 (2020) 26-34.

[9] M. Gao, J.H. Perepezko, Separating β relaxation from α relaxation in fragile metallic glasses based on ultrafast flash differential scanning calorimetry, Phys. Rev. Mater. 4(2) (2020) 025602.

[10] J.S. Harmon, M.D. Demetriou, W.L. Johnson, K. Samwer, Anelastic to plastic transition in metallic glass-forming liquids, Phys. Rev. Lett. 99(13) (2007) 135502.

[11] J.D. Ju, M. Atzmon, A comprehensive atomistic analysis of the experimental

635 dynamic-mechanical response of a metallic glass, Acta Metall. 74 (2014) 183-188.
636 [12] J.C. Qiao, Q. Wang, J. Pelletier, H. Kato, R. Casalini, D. Crespo, E. Pineda, Y.
637 Yao, Y. Yang, Structural heterogeneities and mechanical behavior of amorphous alloys,
638 Prog. Mater. Sci. 104 (2019) 250-329.
639 [13] W.H. Wang, Dynamic relaxations and relaxation-property relationships in
640 metallic glasses, Prog. Mater. Sci. 106 (2019) 100561.
641 [14] A. Furukawa, H. Tanaka, Inhomogeneous flow and fracture of glassy materials,
642 Nat. Mater. 8(7) (2009) 601-609.
643 [15] Z. Lu, W. Jiao, W.H. Wang, H.Y. Bai, Flow unit perspective on room temperature
644 homogeneous plastic deformation in metallic glasses, Phys. Rev. Lett. 113(4) (2014)
645 045501.
646 [16] W. Peter G, Spatiotemporal structures in aging and rejuvenating glasses, Proc.
647 Natl. Acad. Sci. U.S.A. 106(5) (2009) 1353-1358.
648 [17] Y.Q. Cheng, E. Ma, H.W. Sheng, Atomic level structure in multicomponent bulk
649 metallic glass, Phys. Rev. Lett. 102(24) (2009) 245501.
650 [18] Y.H. Liu, T. Fujita, D. Aji, M. Matsuura, M.W. Chen, Structural origins of
651 Johari-Goldstein relaxation in a metallic glass, Nat. Commun. 5(1) (2014) 1-7.
652 [19] Y.H. Liu, D. Wang, K. Nakajima, W. Zhang, A. Hirata, T. Nishi, A. Inoue, M.W.
653 Chen, Characterization of nanoscale mechanical heterogeneity in a metallic glass by
654 dynamic force microscopy, Phys. Rev. Lett. 106(12) (2011) 125504.
655 [20] Q. Wang, J.J. Liu, Y.F. Ye, T.T. Liu, S. Wang, C.T. Liu, J. Lu, Y. Yang, Universal
656 secondary relaxation and unusual brittle-to-ductile transition in metallic glasses, Mater.
657 Today 20(6) (2017) 293-300.
658 [21] Z. Wang, W.H. Wang, Flow units as dynamic defects in metallic glassy materials,
659 NATL SCI REV 6(2) (2019) 304-323.
660 [22] J.M. Pelletier, V.d. Moortèle, Mechanical properties of bulk metallic glasses:
661 Elastic, visco-elastic and visco-plastic components in the deformation, J. Non·Cryst.
662 Solids 353(32-40) (2007) 3750-3753.
663 [23] J.C. Qiao, J.M. Pelletier, Dynamic mechanical relaxation in bulk metallic glasses:
664 a review, J. Mater. Sci. Technol 30(6) (2014) 523-545.

[24] J.C. Qiao, J.M. Pelletier, C. Esnouf, Y. Liu, H. Kato, Impact of the structural state on the mechanical properties in a Zr–Co–Al bulk metallic glass, J. Alloy Compd. 607 (2014) 139-149.

[25] J.C. Qiao, Y. Yao, J.M. Pelletier, L.M. Keer, Understanding of micro-alloying on plasticity in $Cu_{46}Zr_{47-x}Al_7Dy_x$ ($0 \leq x \leq 8$) bulk metallic glasses under compression: based on mechanical relaxations and theoretical analysis, Int. J. Plast. 82 (2016) 62-75.

[26] L.T. Zhang, Y.J. Duan, D. Crespo, E. Pineda, Y.J. Wang, J.M. Pelletier, J.C. Qiao, Dynamic mechanical relaxation and thermal creep of highentropy $La_{30}Ce_{30}Ni_{10}Al_{20}Co_{10}$ bulk metallic glass, Sci. China-Phys. Mech. Astron. 64 (2021) 296111.

[27] G.P. Johari, M. Goldstein, Viscous liquids and the glass transition. II. Secondary relaxations in glasses of rigid molecules, J. Chem. Phys 53(6) (1970) 2372-2388.

[28] X. Monnier, D. Cangialosi, B. Ruta, R. Busch, I. Gallino, Vitrification decoupling from α-relaxation in a metallic glass, Sci. Adv. 6(17) (2020) 1454.

[29] H.B. Yu, W.H. Wang, K. Samwer, The β relaxation in metallic glasses: an overview, Mater. Today 16(5) (2013) 183-191.

[30] F. Zhu, S.X. Song, K.M. Reddy, A. Hirata, M.W. Chen, Spatial heterogeneity as the structure feature for structure–property relationship of metallic glasses, Nat. Commun. 9(1) (2018) 1-7.

[31] P.G. Debenedetti, F.H. Stillinger, Supercooled liquids and the glass transition, Nature (London) 410(6825) (2001) 259-267.

[32] A.S. Argon, Plastic deformation in metallic glasses, Acta Metall. 27(1) (1979) 47-58.

[33] S.G. Mayr, Activation energy of shear transformation zones: A key for understanding rheology of glasses and liquids, Phys. Rev. Lett. 97(19) (2006) 195501.

[34] H.B. Yu, W.H. Wang, H.Y. Bai, Y. Wu, M.W. Chen, Relating activation of shear transformation zones to β relaxations in metallic glasses, Phys. Rev. B 81(22) (2010) 220201.

[35] W.L. Johnson, K. Samwer, A universal criterion for plastic yielding of metallic

695 glasses with a $(T/T_g)^{2/3}$ temperature dependence, Phys. Rev. Lett. 95(19) (2005)
696 195501.
697 [36] Y.Q. Cheng, A.J. Cao, H.W. Sheng, E. Ma, Local order influences initiation of
698 plastic flow in metallic glass: Effects of alloy composition and sample cooling history,
699 Acta Metall. 56(18) (2008) 5263-5275.
700 [37] D. Granata, E. Fischer, J.F. Löffler, Effectiveness of hydrogen microalloying in
701 bulk metallic glass design, Acta Metall. 99 (2015) 415-421.
702 [38] L.S. Luo, B.B. Wang, F.Y. Dong, Y.Q. Su, E.Y. Guo, Y.J. Xu, M.Y. Wang, L.
703 Wang, J.X. Yu, R. Ritchie, Structural origins for the generation of strength, ductility
704 and toughness in bulk-metallic glasses using hydrogen microalloying, Acta Metall.
705 171 (2019) 216-230.
706 [39] N. Nollmann, I. Binkowski, V. Schmidt, H. Rösner, G. Wilde, Impact of
707 micro-alloying on the plasticity of Pd-based bulk metallic glasses, Scr. Mater. 111
708 (2016) 119-122.
709 [40] H.B. Yu, K. Samwer, W.H. Wang, H.Y. Bai, Chemical influence on β-relaxations
710 and the formation of molecule-like metallic glasses, Nat. Commun. 4(1) (2013) 1-6.
711 [41] B. Sarac, Y.P. Ivanov, A. Chuvilin, T. Schöberl, M. Stoica, Z.L. Zhang, J. Eckert,
712 Origin of large plasticity and multiscale effects in iron-based metallic glasses, Nat.
713 Commun. 9(1) (2018) 1-10.
714 [42] D. Şopu, S. Scudino, X.L. Bian, C. Gammer, J. Eckert, Atomic-scale origin of
715 shear band multiplication in heterogeneous metallic glasses, Scr. Mater. 178 (2020)
716 57-61.
717 [43] M. Bletry, P. Guyot, J.-J. Blandin, J.-L. Soubeyroux, Free volume model:
718 High-temperature deformation of a Zr-based bulk metallic glass, Acta Metall. 54(5)
719 (2006) 1257-1263.
720 [44] M.H. Cohen, D. Turnbull, Molecular transport in liquids and glasses, J. Chem.
721 Phys 31(5) (1959) 1164-1169.
722 [45] F. Spaepen, A microscopic mechanism for steady state inhomogeneous flow in
723 metallic glasses, Acta Metallurgica 25(4) (1977) 407-415.
724 [46] W. Jiao, P. Wen, H. Peng, H.Y. Bai, B.A. Sun, W.H. Wang, Evolution of

725 structural and dynamic heterogeneities and activation energy distribution of
726 deformation units in metallic glass, Appl. Phys. Lett. 102(10) (2013) 101903.
727 [47] Z. Wang, B.A. Sun, H.Y. Bai, W.H. Wang, Evolution of hidden localized flow
728 during glass-to-liquid transition in metallic glass, Nat. Commun. 5 (2014) 5823.
729 [48] A. Granato, Interstitialcy model for condensed matter states of
730 face-centered-cubic metals, Phys. Rev. Lett. 68(7) (1992) 974.
731 [49] A.V. Granato, Interstitialcy theory of simple condensed matter, EUR. PHYS. J. B
732 87(1) (2014) 1-6.
733 [50] D.N. Perera, A.P. Tsai, Dynamic tensile measurements for below the calorimetric
734 glass transition temperature, Journal of Physics: Condensed Matter 11(15) (1999)
735 3029.
736 [51] J. Perez, Quasi-punctual defects in vitreous solids and liquid-glass transition,
737 Solid State Ionics 39(1) (1990) 69-79.
738 [52] J. Perez, J.Y. Cavaille, Temperature dependence of the molecular dynamics in
739 amorphous polymers through the rubber-glass transition, J. Non·Cryst. Solids 172
740 (1994) 1028-1036.
741 [53] R. Rinaldi, R. Gaertner, L. Chazeau, C. Gauthier, Modelling of the mechanical
742 behaviour of amorphous glassy polymer based on the Quasi Point Defect
743 theory—Part I: Uniaxial validation on polycarbonate, Int. J. Nonlin. Mech. 46(3)
744 (2011) 496-506.
745 [54] J.M. Pelletier, J. Perez, L. Duffrene, Mechanical response of an oxide glass to
746 mechanical loading—shear and volume relaxation effects: physical analysis, Acta
747 Metall. 48(6) (2000) 1397-1408.
748 [55] S. Etienne, J.Y. Cavaillé, J. Perez, R. Point, M. Salvia, Automatic system for
749 analysis of micromechanical properties, Rev. Sci. Instrum. 53(8) (1982) 1261-1266.
750 [56] Y.T. Cheng, Q. Hao, J.C. Qiao, D. Crespo, E. Pineda, J.M. Pelletier, Effect of
751 minor addition on dynamic mechanical relaxation in ZrCu-based metallic glasses, J.
752 Non·Cryst. Solids (2020) 120496.
753 [57] J.C. Qiao, Y.X. Chen, J.M. Pelletier, H. Kato, D. Crespo, Y. Yao, V.A. Khonik,
754 Viscoelasticity of Cu-and La-based bulk metallic glasses: Interpretation based on the

quasi-point defects theory, Mater. Sci. Eng. A 719 (2018) 164-170.
[58] Z.F. Zhao, P. Wen, C.H. Shek, W.H. Wang, Measurements of slow β-relaxations in metallic glasses and supercooled liquids, Phys. Rev. B 75(17) (2007) 174201.
[59] C.A. Angell, Formation of glasses from liquids and biopolymers, Science 267(5206) (1995) 1924-1935.
[60] Z.F. Yao, J.C. Qiao, J.M. Pelletier, Y. Yao, Characterization and modeling of dynamic relaxation of a Zr-based bulk metallic glass, J. Alloy Compd. 690 (2017) 212-220.
[61] A. Takeuchi, A. Inoue, Calculations of mixing enthalpy and mismatch entropy for ternary amorphous alloys, Mater. T. JIM 41(11) (2000) 1372-1378.
[62] A. Takeuchi, A. Inoue, Classification of bulk metallic glasses by atomic size difference, heat of mixing and period of constituent elements and its application to characterization of the main alloying element, Mater. Trans. 46(12) (2005) 2817-2829.
[63] J.Y. Cavaille, J. Perez, G.P. Johari, Molecular theory for the rheology of glasses and polymers, Phys. Rev. B 39(4) (1989) 2411.
[64] J.Y. Cavaillé, J. Perez, G.P. Johari, A comparison of a point defects theory with mechanical relaxations in polymers, J. Non·Cryst. Solids 131 (1991) 935-941.
[65] M.B.M. Mangion, J.Y. Cavaille, J. Perez, A molecular theory for the sub-Tg plastic mechanical response of amorphous polymers, Philos. Mag. A 66(5) (1992) 773-796.
[66] R.G. Palmer, D.L. Stein, E. Abrahams, P.W. Anderson, Models of hierarchically constrained dynamics for glassy relaxation, Phys. Rev. Lett. 53(10) (1984) 958.
[67] C. Gauthier, J.M. Pelletier, L. David, G. Vigier, J. Perez, Relaxation of non-crystalline solids under mechanical stress, J. Non·Cryst. Solids 274(1-3) (2000) 181-187.
[68] J.M. Pelletier, B. Van de Moortèle, I. Lu, Viscoelasticity and viscosity of Pd–Ni–Cu–P bulk metallic glasses, Mater. Sci. Eng. A 336(1-2) (2002) 190-195.
[69] Q. Wang, J.M. Pelletier, Y.D. Dong, Y.F. Ji, Structural relaxation and crystallisation of bulk metallic glasses $Zr_{41}Ti_{14}Cu_{12.5}Ni_{10-x}Be_{22.5}Fe_x$ (x= 0 or 2) studied by mechanical spectroscopy, Mater. Sci. Eng. A 370(1-2) (2004) 316-320.

[70] L.S. Huo, J.F. Zeng, W.H. Wang, C.T. Liu, Y. Yang, The dependence of shear modulus on dynamic relaxation and evolution of local structural heterogeneity in a metallic glass, Acta Metall. 61(12) (2013) 4329-4338.

[71] T.J. Lei, L.R. DaCosta, M. Liu, J. Shen, Y.H. Sun, W.H. Wang, M. Atzmon, Composition dependence of metallic glass plasticity and its prediction from anelastic relaxation–A shear transformation zone analysis, Acta Metall. 195 (2020) 81-86.

[72] H.B. Yu, X. Shen, Z. Wang, L. Gu, W.H. Wang, H.Y. Bai, Tensile plasticity in metallic glasses with pronounced β relaxations, Phys. Rev. Lett. 108(1) (2012) 015504.

[73] A. Taub, F. Spaepen, The kinetics of structural relaxation of a metallic glass, Acta Metall. 28(12) (1980) 1781-1788.

[74] S. Tsao, F. Spaepen, Structural relaxation of a metallic glass near equilibrium, Acta Metall. 33(5) (1985) 881-889.

[75] J.C. Qiao, Y.J. Wang, J.M. Pelletier, L.M. Keer, M.E. Fine, Y. Yao, Characteristics of stress relaxation kinetics of $La_{60}Ni_{15}Al_{25}$ bulk metallic glass, Acta Metall. 98 (2015) 43-50.

[76] A. Slipenyuk, J. Eckert, Correlation between enthalpy change and free volume reduction during structural relaxation of $Zr_{55}Cu_{30}Al_{10}Ni_5$ metallic glass, Scr. Mater. 50(1) (2004) 39-44.

[77] J.C. Qiao, R. Casalini, J.M. Pelletier, H. Kato, Characteristics of the structural and Johari–Goldstein relaxations in Pd-based metallic glass-forming liquids, J. Phys. Chem. B 118(13) (2014) 3720-3730.

[78] H.T. Jeong, J.M. Park, W.T. Kim, D.H. Kim, Quasicrystalline effects on the mechanical relaxation behavior of a $Ti_{45}Zr_{16}Ni_9Cu_{10}Be_{20}$ metallic glass, Mater. Sci. Eng. A 527(1-2) (2009) 1-6.

[79] G. Williams, D.C. Watts, Non-symmetrical dielectric relaxation behaviour arising from a simple empirical decay function, Trans. Faraday Society 66 (1970) 80-85.

[80] R. Bergman, General susceptibility functions for relaxations in disordered systems, J. Appl. Phys. 88(3) (2000) 1356-1365.

[81] Q. Wang, J.M. Pelletier, J. Lu, Y.D. Dong, Study of internal friction behavior in a

815 Zr base bulk amorphous alloy around the glass transition, Mater. Sci. Eng. A 403(1-2)
816 (2005) 328-333.
817 [82] N. Ouali, M. Mangion, J. Perez, Experimental and theoretical analysis of both the
818 small-and the large-stress mechanical response of poly (methyl methacrylate), Philos.
819 Mag. A 67(4) (1993) 827-848.
820

821 **Captions of figures:**

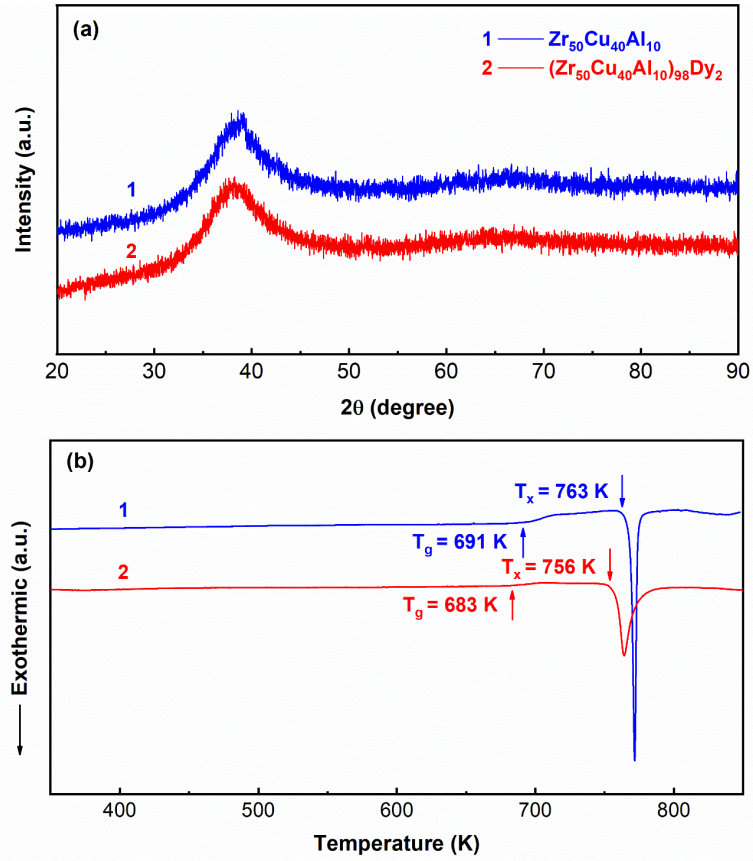

822

823 **Fig.1** (a) The typical XRD patterns and (b) DSC curves of $(Zr_{50}Cu_{40}Al_{10})_{100-x}Dy_x$ (x=0

824 or 2) bulk metallic glasses (heating rate is 10 K/min).

825

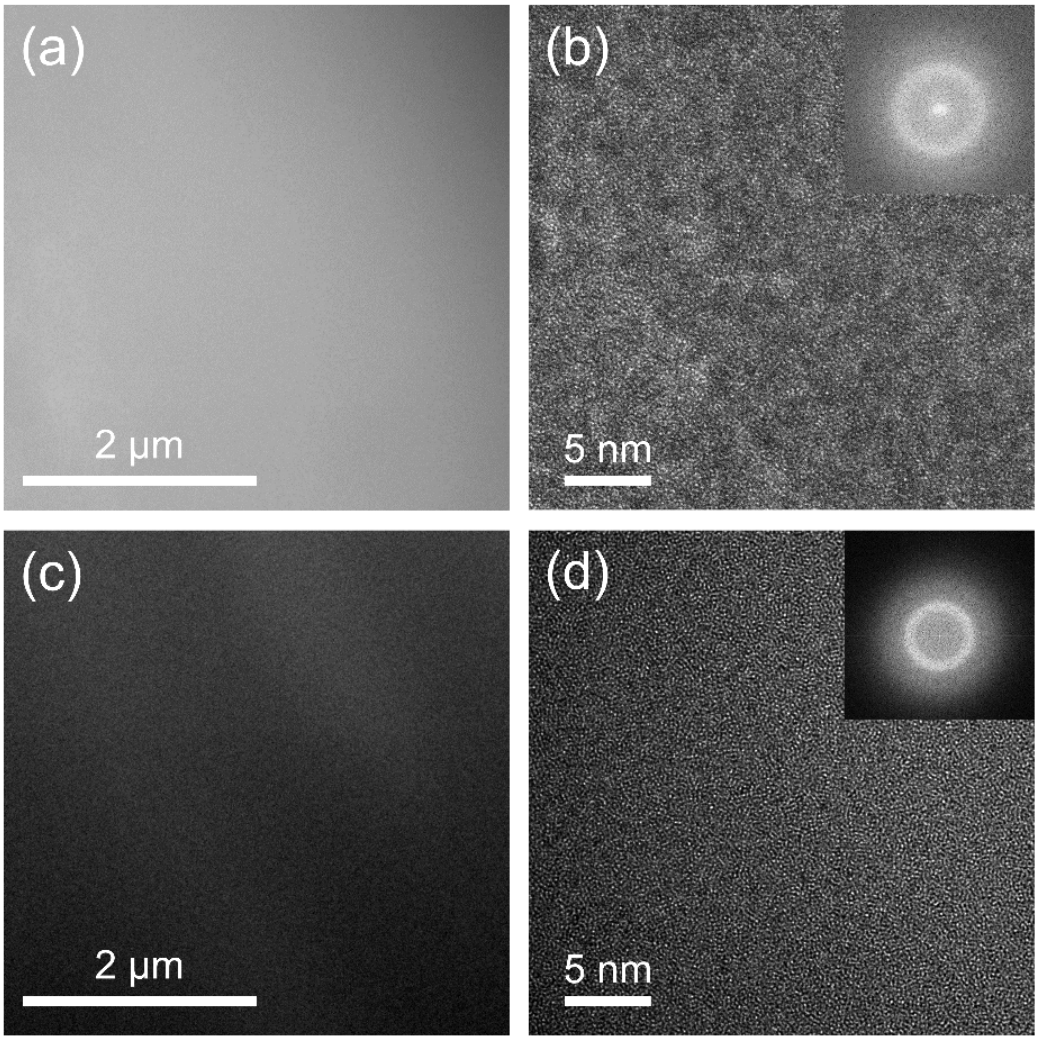

826

827 **Fig.2** (a) TEM micrograph and (b) HRTEM image of as-cast $Zr_{50}Cu_{40}Al_{10}$ metallic
828 glass. (c) TEM micrograph and (d) HRTEM image of $(Zr_{50}Cu_{40}Al_{10})_{98}Dy_2$ metallic
829 glass. Insets in (b) and (d) showing the corresponding FFT images.

830

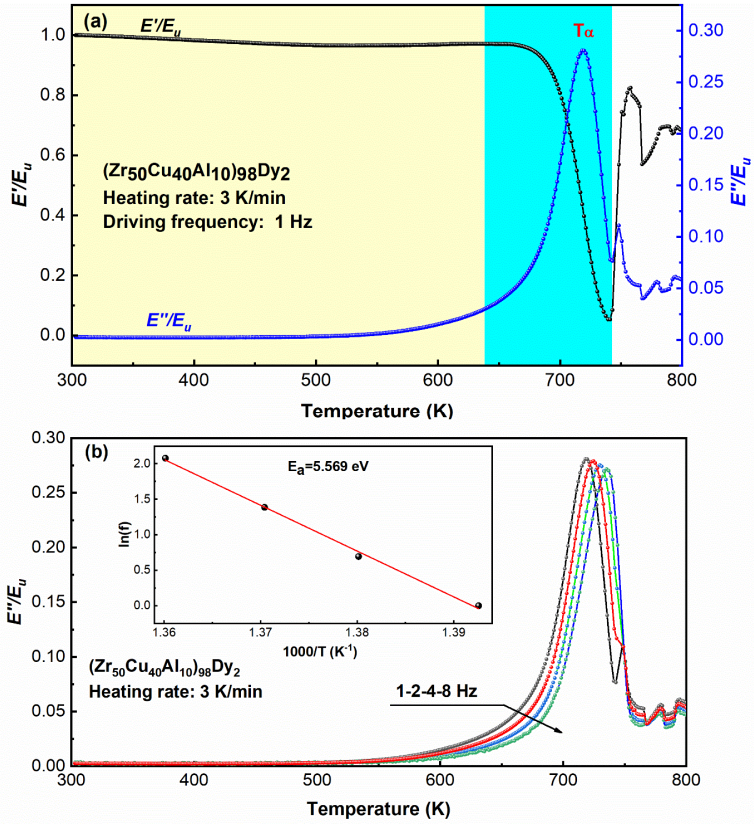

Fig.3 (a) Normalized storage modulus and loss modulus of $(Zr_{50}Cu_{40}Al_{10})_{98}Dy_2$ metallic glass as function of the temperature; (b) The normalized loss modulus as function of the temperature of $(Zr_{50}Cu_{40}Al_{10})_{98}Dy_2$ metallic glass with different driving frequency. Inset is the Arrhenius relation of peak frequency of loss modulus *versus* the reciprocal of temperature.)

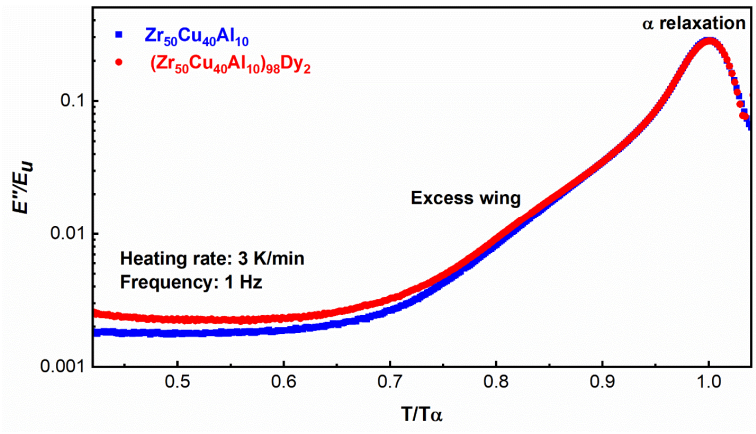

838

839 **Fig.4** Temperature dependence of the normalized loss modulus E''/E_u in the

840 $(Zr_{50}Cu_{40}Al_{10})_{100-x}Dy_x$ (x=0 or 2) metallic glasses.

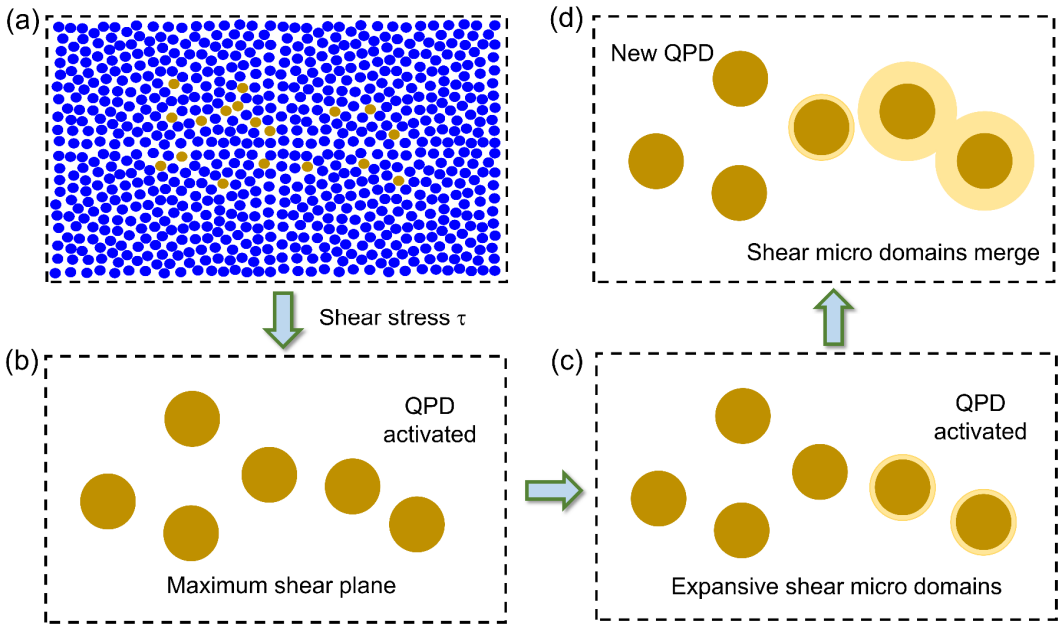

841

842 **Fig.5** Conceptual description of the microstructural arrangements within a glassy
843 amorphous materialas posted by the QPD model: (a) original configuration of the
844 glassy state, the golden and blue balls represent quasi point defests and elestic matrix,
845 respectively, (b,c,d) micro structural reorganization (activation of these QPD and
846 growth of sheared micro domains) provoked by an external thermomechanical
847 stimuli.

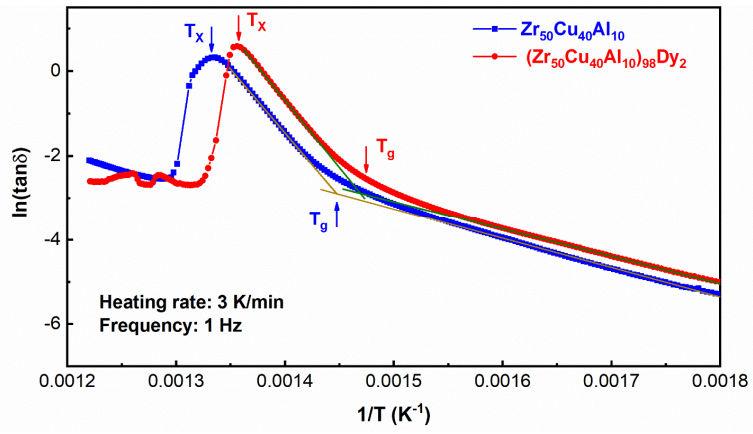

848

849 **Fig.6** Logarithm of the internal friction ln(tan δ) *versus* reciprocal of the

850 temperature $1/T$ of the $(Zr_{50}Cu_{40}Al_{10})_{100-x}Dy_x$ (x=0 or 2) bulk metallic glasses.

851

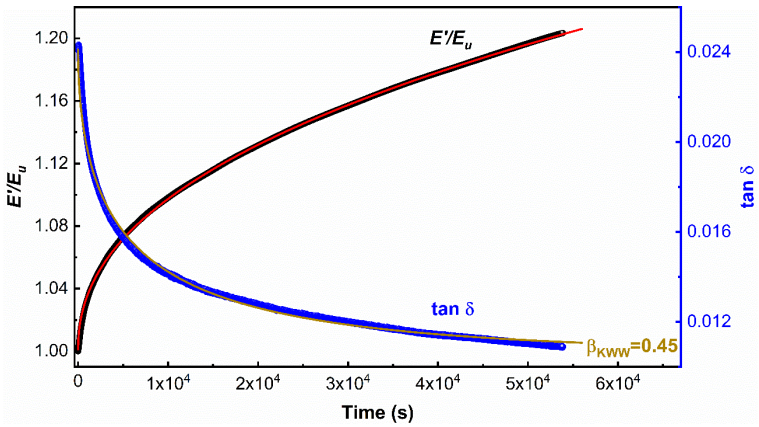

852

853 **Fig.7** Evolution of the storage modulus E'/E_u and the loss factor tan δ with the
854 aging time at 625 K in the $(Zr_{50}Cu_{40}Al_{10})_{98}Dy_2$ metallic glass. The solid lines are
855 fitted by the KWW equation of the **Eq.(12)**.

856

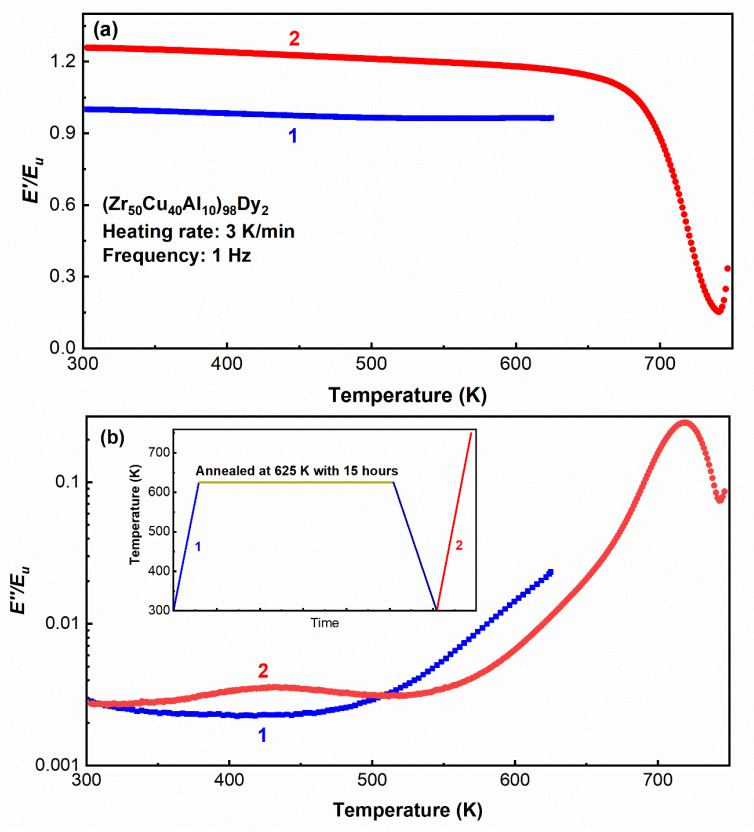

857

858 **Fig.8** Effect of the physical aging below the glass transition temperature on the
859 dynamic mechanical behavior of the $(Zr_{50}Cu_{40}Al_{10})_{98}Dy_2$ metallic glass. (a)
860 Normalized storage modulus of $(Zr_{50}Cu_{40}Al_{10})_{98}Dy_2$ metallic glass at as-cast state and
861 annealed state. (b) Normalized loss modulus of $(Zr_{50}Cu_{40}Al_{10})_{98}Dy_2$ metallic glass at
862 as-cast state and annealed state.

863

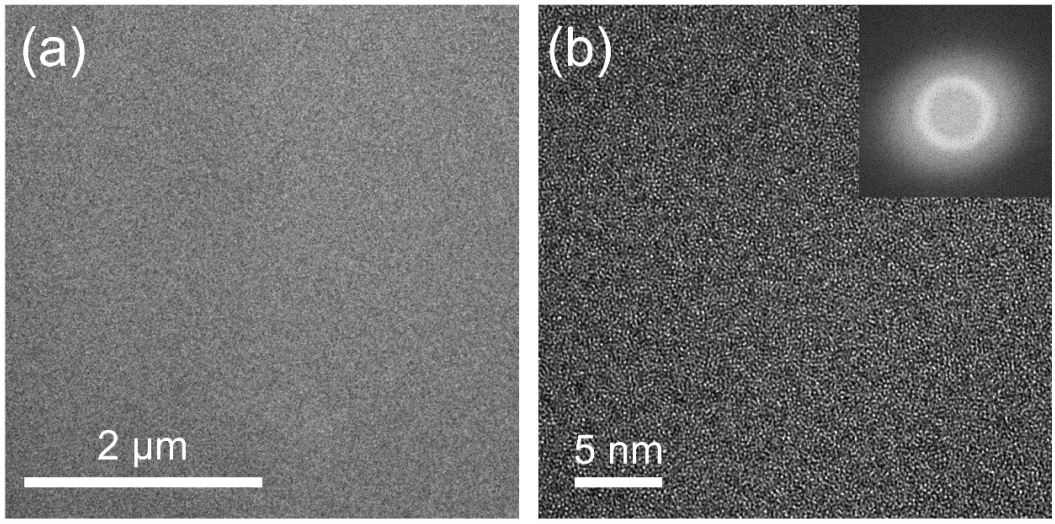

Fig.9 (a) TEM micrograph and (b) HRTEM image of the annealed $(Zr_{50}Cu_{40}Al_{10})_{98}Dy_2$ metallic glass with an inset in (b) showing the corresponding FFT image.

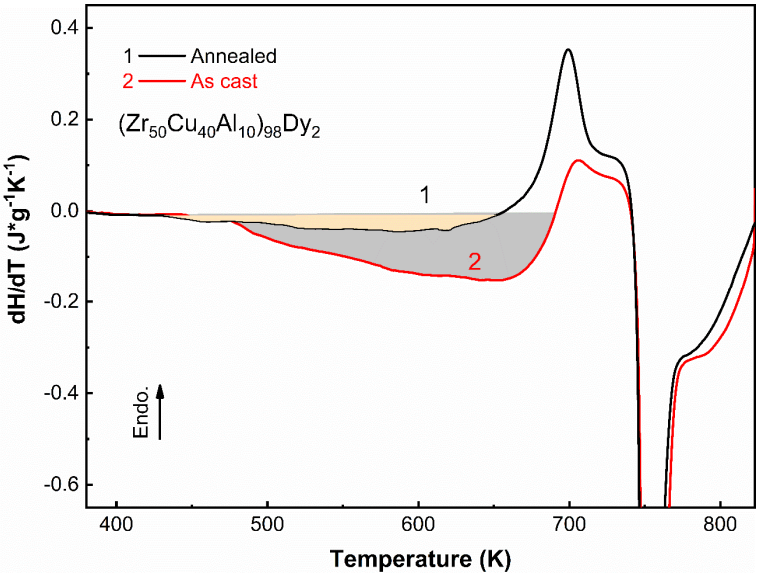

869

870 **Fig.10** Relaxation enthalpy from the differential scanning calorimetry traces of
871 $(Zr_{50}C_{40}Al_{10})_{98}Dy_2$ bulk metallic glass: as-cast state and annealed sample (annealing
872 temperature T_a is 625 K with annealing time is 15 h). The relaxation enthalpy (ΔH)
873 gradually decreases after annealing below the glass transition temperature T_g.

874

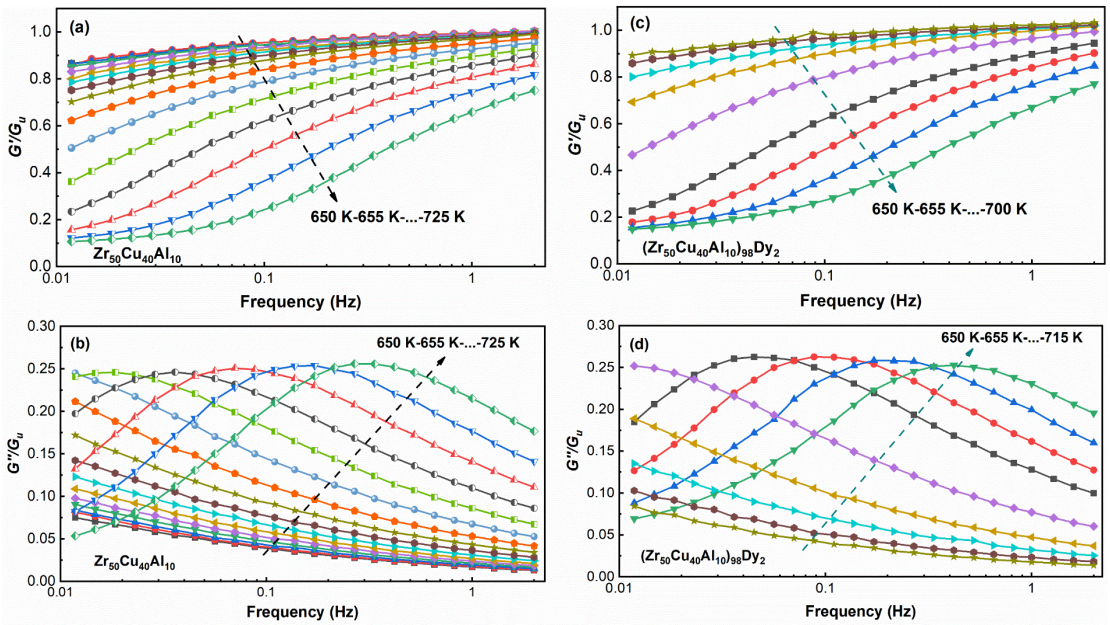

Fig.11 Normalized shear modulus as a function of frequency at different temperature of $(Zr_{50}Cu_{40}Al_{10})_{100-x}Dy_x$ (x=0 or 2) bulk metallic glasses: (a) Storage modulus G'/G_u of $Zr_{50}Cu_{40}Al_{10}$ metallic glass and (b) Loss modulus G''/G_u of$Zr_{50}Cu_{40}Al_{10}$ metallic glass, (c) Storage modulus G'/G_u of $(Zr_{50}Cu_{40}Al_{10})_{98}Dy_2$ metallic glass and (d) Loss modulus G''/G_u of $(Zr_{50}Cu_{40}Al_{10})_{98}Dy_2$ metallic glass.

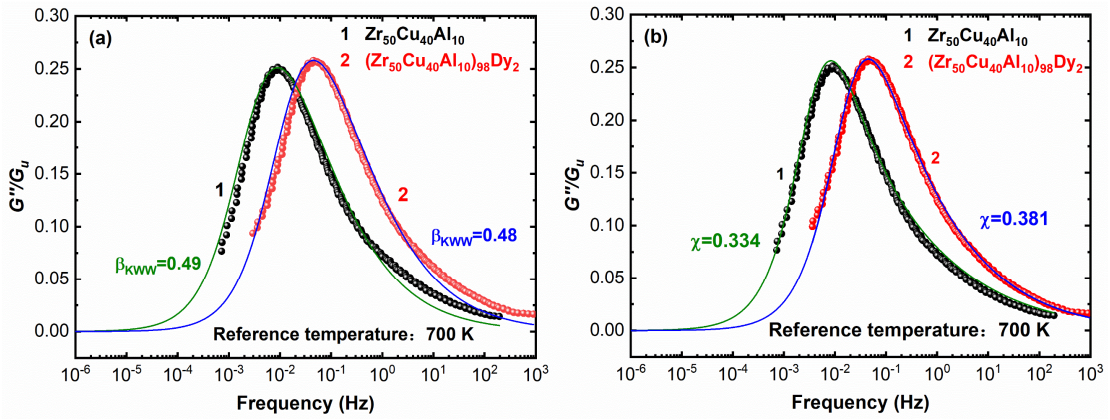

882

883 **Fig.12** The master curves of the normalized loss modulus G''/G_u of the

884 $(Zr_{50}Cu_{40}Al_{10})_{100-x}Dy_x$ (x=0 or 2) bulk metallic glasses. The reference temperature is

885 700 K. (a) The solid lines are fitted by the **Eq.(17)** of KWW equation; (b) The solid

886 lines are fitted by the **Eq.(9)** of QPD theory.

887

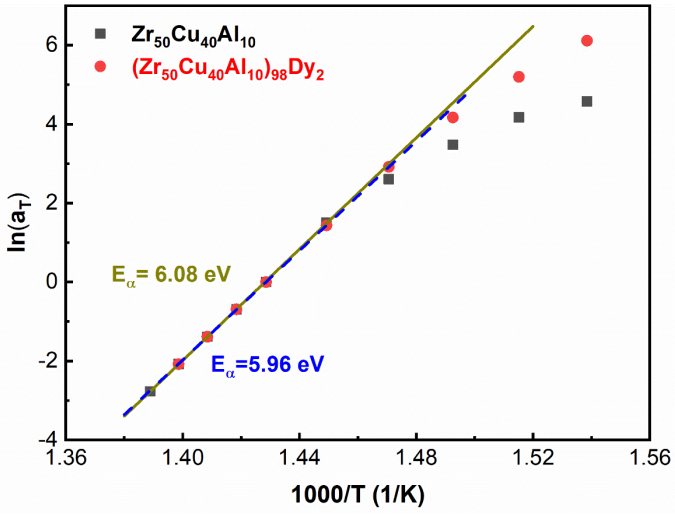

888

889 **Fig.13** Temperature dependence of the shift factor for the $(Zr_{50}Cu_{40}Al_{10})_{100-x}Dy_x$ (x=0

890 or 2) bulk metallic glasses. The apparent activation energy E_α of the α relaxation

891 process was marked in the figure (the fitting lines are the Arrhenius plots).

892

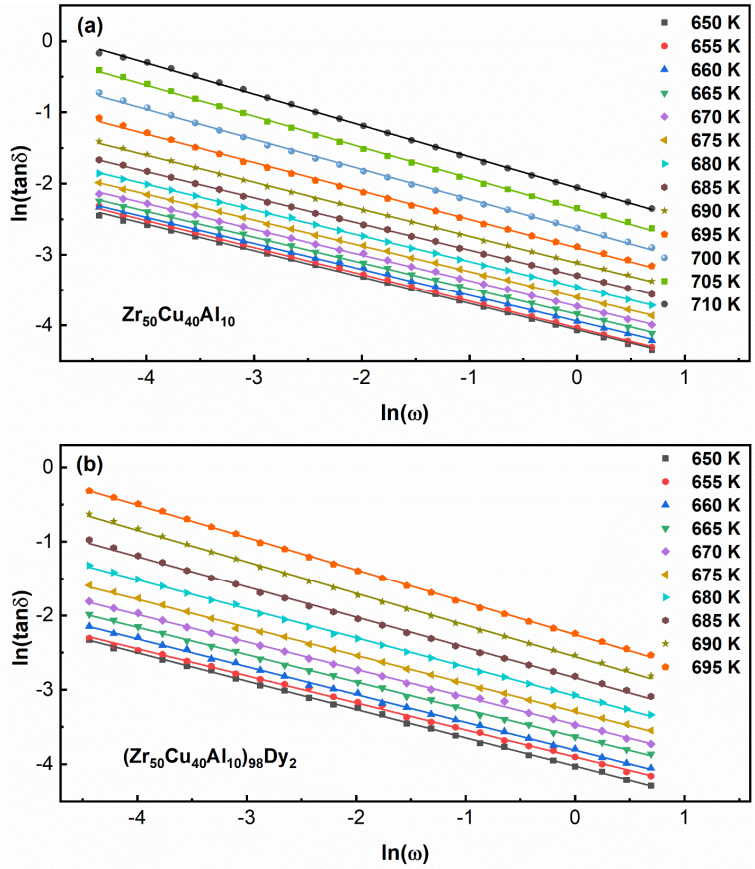

893

894 **Fig.14** Effect of the driving frequency on the loss factor tan δ at various

895 temperature of $Zr_{50}Cu_{40}Al_{10}$ metallic glass (a) and $(Zr_{50}Cu_{40}Al_{10})_{98}Dy_2$ metallic glass

896 (b). Solid lines are fitted by the **Eq.(10)**.

897

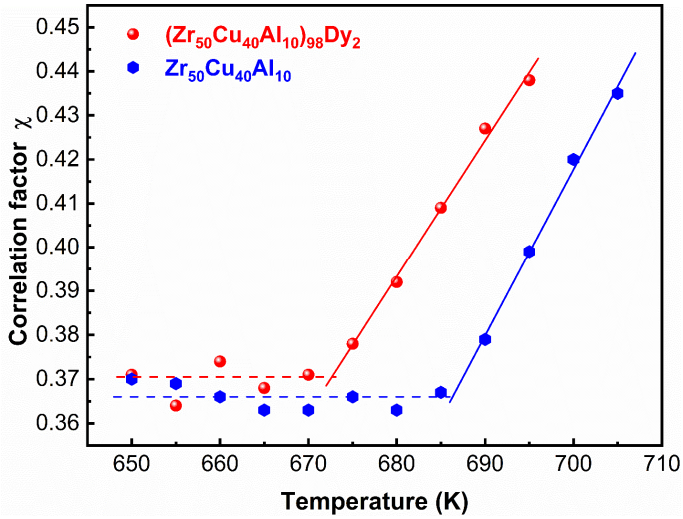

898

899 **Fig.15** The correlation factor χ as a function of temperature of the

900 $(Zr_{50}Cu_{40}Al_{10})_{100-x}Dy_x$ (x=0 or 2) bulk metallic glasses.

901

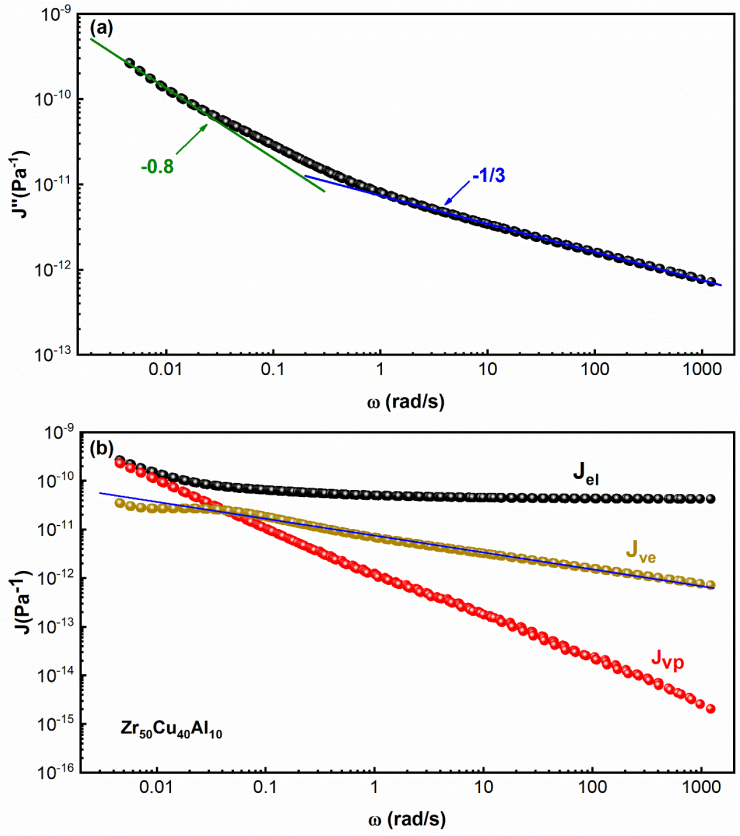

Fig.16 (a) Imaginary compliance *versus* the angular frequency of $Zr_{50}Cu_{40}Al_{10}$ metallic glass; (b) Different components of the compliance J as a function of the angular frequency ω. The reference temperature is 700 K.

Graphical Abstract